An intense ultraviolet photoluminescence in sol–gel ZnO–SiO$_2$ nanocomposites

Zhengping Fu, Beifang Yang[1]**, Lin Li, Weiwei Dong, Chong Jia and Wan Wu**

Department of Materials Science and Engineering, University of Science and Technology of China, Hefei 230026, People's Republic of China

E-mail: bfyang@ustc.edu.cn

Abstract
We report the phenomenon that the intensity of the ultraviolet (UV) photoluminescence (PL) from ZnO was greatly enhanced by incorporating ZnO into the SiO$_2$ matrix. PL excitation results show that both the ZnO nanoparticles and the SiO$_2$ matrix in the nanocomposites contribute to the luminescence process for the UV band. On the basis of the x-ray photoelectron spectra, we suggest that interface energy states are formed due to the presence of Zn–O–Si bonds between ZnO nanoparticles and the SiO$_2$ matrix. A tentative model concerning the contribution of the ZnO nanoparticles, SiO$_2$ matrix, and ZnO–SiO$_2$ interface is suggested to explain the PL enhancement effect.

1. Introduction

ZnO-based nanocomposites are promising materials for electroluminescent applications such as in flat-panel displays, photoelectronics integrated devices, and semiconductor lasers. However, the luminescence efficiency of ZnO-based nanocomposites needs to be improved for the above applications. Recently, a number of research groups have demonstrated that the green–yellow emissions are enhanced in ZnO-based nanocomposites [1–8]. However, the luminescence efficiency of the ultraviolet (UV) band in ZnO, which is very attractive in view of possible applications [9], is not high enough because most of the excited carriers do not recombine via exciton transition, but recombine at deeply trapped defects in ZnO [10]. To our knowledge, few studies have been done on the UV photoluminescence (PL) in ZnO-based nanocomposites. Yao *et al* [11] reported band gap luminescence from ZnO in mesoporous silica, and they proposed that Zn–O–Si cross-linking bonds that formed at the interface between ZnO and the pore walls of silica had a great influence on the optical properties of ZnO/SiO$_2$. In this work, we incorporated ZnO nanoparticles into a SiO$_2$ matrix by the sol–gel method and found that the intensity of the UV PL band was greatly enhanced as compared to that of ZnO.

---

[1] Author to whom any correspondence should be addressed.

We suggest that the ZnO nanoparticles and SiO_2 matrix, as well as the ZnO–SiO_2 interface, are responsible for the UV PL enhancement effect.

2. Experiment

The nanosized ZnO sample was prepared by the sol–gel [12] method: zinc acetate, $Zn(CH_3COO)_2 \cdot 2H_2O$ (AR grade), and absolute ethanol (AR grade) were used in the synthesis without further purification. A 0.1 M ethanolic solution of zinc acetate was prepared by dissolving 0.015 mol of zinc acetate in 150 ml of ethanol in a 250 ml round-bottom distillation flask. The flask was fitted with a condenser and refluxed while stirring for 3 h at 80 °C. At the end of this procedure, 150 ml of reaction product was obtained. Then, 0.02 mol of lithium hydroxide powder ($LiOH \cdot H_2O$) was added to this precursor to give a final lithium concentration of 0.14 M. The mixture was then hydrolysed in an ultrasonic bath to accelerate the reaction. This hydrolysis reaction was continued at room temperature until lithium hydroxide powder was no longer visibly present (about 8 h). White precipitate (ZnO colloidal aggregation) was obtained by adding hexane into the solution. The supernatant was discarded, and the precipitate was re-dispersed in absolute ethanol and subjected recursively to this gentle precipitation procedure three times. The ZnO colloid prepared by these procedures was quite stable, and no precipitate was noticed even after three weeks of storage in a refrigerator. The powder sample for x-ray diffraction (XRD) measurements was prepared by drying the colloid at room temperature.

The ZnO–SiO_2 composite powder was prepared by the sol–gel method. First 5 ml of absolute alcohol, 5 ml of $Si(OEt)_4$, and some $Zn(NO_3)_2$ were mixed together in a 25 ml conical flask to make a homogeneous solution (Zn/Si mole ratio 1:10). Then 0.8 ml of 0.01 M HCl aqueous solution was slowly dropped into the flask at room temperature while stirring. The solution was refluxed at 69 °C for 2 h to form the sol. After the sol had been aged at room temperature for 24 h, 10 ml of absolute alcohol was added into the sol; this was followed by 10 min of stirring. The sol was dried at 60 °C in an oven and then calcined at 600 °C for 2 h in air to produce the ZnO–SiO_2 composite. For comparison, a SiO_2 sample was prepared by the same route as for the ZnO–SiO_2 composite, except that no $Zn(NO_3)_2$ was added.

The powder XRD was measured on a D/max-y A rotating anode x-ray diffractometer by spreading the sample on the specimen holder with alcohol. The PL and photoluminescence excitation (PLE) spectra of all the samples were taken on a Hitachi-850 fluorescence spectrophotometer. The light source used was a 300 W Xe lamp. The spectra of the SiO_2 matrix were subtracted by computer analysis from the measured excitation and emission spectra of the ZnO–SiO_2 composite. The x-ray photoelectron spectra (XPS) measurements were carried out on a VG ESCALAB mark II spectrometer. A Mg Kα source (1253.6 eV photons) was used with the analyser mode set at a constant analyser energy of 20 eV. The x-ray source was run at 150 W (15 kV and 10 mA). The microstructure of the ZnO–SiO_2 composite was observed by high-resolution transmission electron microscopy (HRTEM) (JEOL-2010) at 200 kV. For HRTEM sample preparation, the composite was ground in an agate mortar and ultrasonically dispersed in ethanol; a drop was then dripped onto carbon-coated Cu micro-grids. All the measurements were conducted at room temperature.

3. Results and discussion

The XRD spectra of the ZnO and ZnO–SiO_2 samples are shown in figure 1. The ZnO powder is crystalline and the grain size calculated from Scherrer equations is about 4 nm. The ZnO–SiO_2 powder shows an amorphous nature, and the formation of ZnO–SiO_2 nanocomposites is confirmed by the HRTEM micrograph, which is illustrated as the inset in figure 1. The
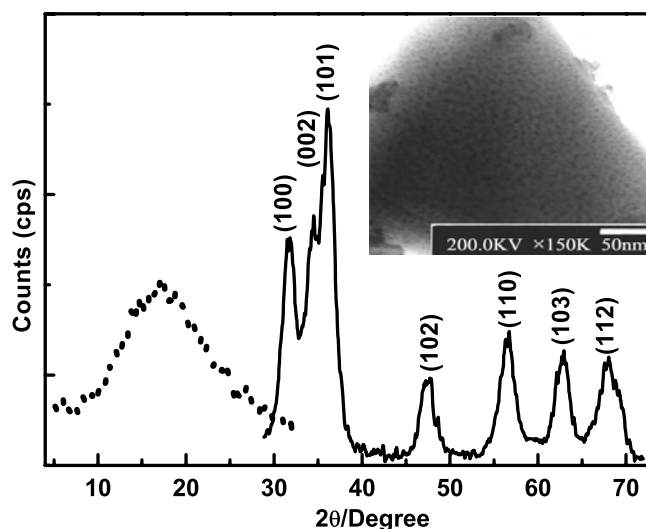
Figure 1. XRD spectra of the ZnO sample (solid curve) and the ZnO–SiO$_2$ sample (dotted curve). The inset shows the HREM micrograph for the ZnO–SiO$_2$ sample; SiO$_2$ and ZnO were discriminated as the white background and black dots, respectively, by atomic-number-produced contrast during the observation.

possible existence of Zn$_2$SiO$_4$ is ruled out [13], for Zn$_2$SiO$_4$ is formed at calcining temperatures >900 °C. It can be seen that the ZnO nanoparticles were homogeneously distributed in the SiO$_2$ matrix. The average size of the ZnO particles in the composite is about 3–6 nm as measured from the HRTEM micrograph. The absence of a lattice fringe in the HRTEM micrograph also confirms that both the ZnO particles and the SiO$_2$ matrix in the composite sample are amorphous, which is consistent with the x-ray powder diffraction results.

Under excitation with 277 nm light, the PL spectra of the ZnO sample consist of a broad visible band centred at 582 nm and a very weak UV band centred at 365 nm (curve (a) in figure 2), which are for the defect state emission and the near-band-edge (NBE) emission respectively [14]. With a 235 nm exciting source light, an enhanced UV broad band was observed from the ZnO–SiO$_2$ composites (curve (b) in figure 2). In the PL spectra of the ZnO–SiO$_2$ sample there are a main broad UV band centred at 380 nm with two inconspicuous shoulders centred at 350 and 470 nm, while the visible emission band at 582 nm is very weak. For comparison, we define the ratio $R = I_{UV}/I_{VIS}$ as the ratio of the intensity of the UV emission to that of the visible emission at room temperature. The effect of the nanocomposite structure on the UV PL process is obvious: R for the ZnO–SiO$_2$ sample is much greater than that for the ZnO sample. The relation of and/or differences between the UV PL processes for these two types of sample are more evident in the PLE spectra which were measured by monitoring the UV emission band. The results are illustrated in figure 3. The PLE spectra of the ZnO samples show a wide band at 260–340 nm, which is due to the process in which carriers are excited in ZnO nanoparticles [15]. On the other hand, the PLE spectra of the ZnO–SiO$_2$ samples contain not only a 260–340 nm band, but also a stronger band at 230 nm, which may originate from the SiO$_2$ matrix [16]. This result implies that in the nanocomposites there are several mechanisms entangled in the UV emission, i.e. all of the ZnO nanoparticles, the ZnO–SiO$_2$ interface, and the SiO$_2$ matrix contributed to the UV emission.

To reveal the electric state in the nanocomposites, XPS of the samples were measured and these are shown in figure 4. The binding energy of the Zn$_{2P}$ electron ($E_{B,2P}$) in the ZnO–SiO$_2$
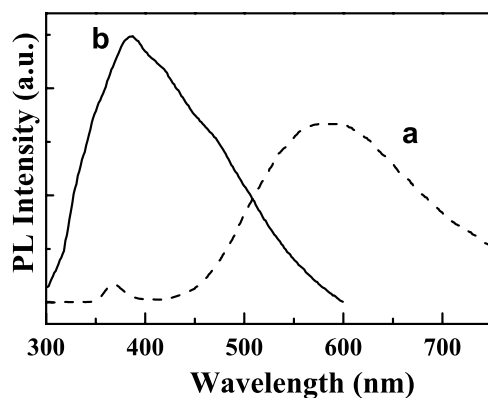
Figure 2. PL spectra of (a) ZnO excited with 277 nm light and (b) ZnO–SiO$_2$ excited with 235 nm light.
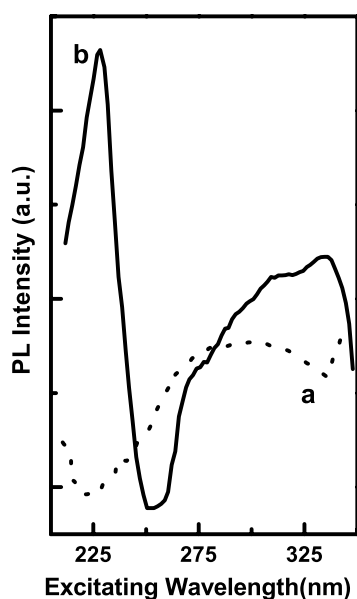

Figure 3. PLE spectra of (a) the 365 nm peak of ZnO and (b) the 380 nm peak of ZnO–SiO$_2$.

composite is 1.9 eV higher than that in pure ZnO, while the kinetic energy of the Auger Zn L$_3$M$_{4,5}$M$_{4,5}$ electron ($E_{k,LMM}$) in ZnO–SiO$_2$ is 3.05 eV lower than that in pure ZnO [17]. The increase in binding energy and the decrease in kinetic energy of the Auger electron are both related to the decrease in valence electron density. The modified Auger parameter (α), which is usually defined as $\alpha = E_{k,LMM} + E_{B,2P}$ for Zn, is a good measure for identifying the chemical state [18]. α is 2009.1 eV for ZnO–SiO$_2$ composite as compared with 2010.25 eV for pure ZnO. The difference in Auger parameter is attributed to the difference in extra-atomic relaxation energy due to the difference in chemical state. Due to the electronegativity of Si ($\sim$1.9) being higher than that of Zn ($\sim$1.65), the valence electron density of Zn in the Zn–O–Si bond is lower than that in the Zn–O–Zn bond [7], which makes it reasonable to ascribe the shifts of $E_{B,2P}$, $E_{k,LMM}$, and the Auger parameter to the formation of Zn–O–Si.
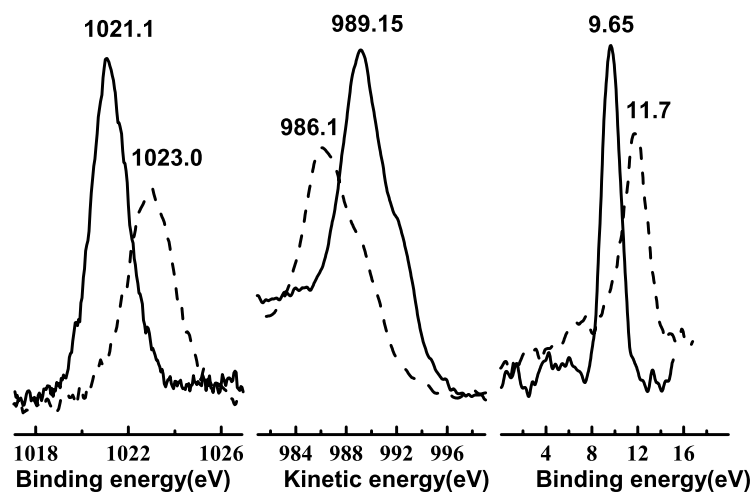
Figure 4. Zn$_{2P}$ (a), L$_3$M$_{4,5}$M$_{4,5}$ (b), and Zn 3d (c) spectra of pure ZnO (solid curve) and ZnO–SiO$_2$ composites (dashed curve). The shifts of the peaks for ZnO–SiO$_2$ composites indicate the formation of Zn–O–Si bonds at the ZnO–SiO$_2$ interface.

On the other hand, previous calculations [19–22] have shown that Zn$_{3d}$ electrons as well as Zn$_{4s}$ and Zn$_{4p}$ electrons participate in the covalent binding between zinc and oxygen atoms in ZnO. For nanoparticles with sizes of several nanometres, the XPS spectra are dominated by atoms at the nanoparticle surface, and a shift of the Zn$_{3d}$ peak is expected if a Zn–O–Si bond is in fact formed in the interface. We present the resulting Zn$_{3d}$ spectrum in figure 4(c). As expected, the binding energy of the Zn$_{3d}$ electron did in fact shift from 9.65 eV for pure ZnO to 11.7 eV for ZnO–SiO$_2$ composite. Therefore, the XPS results suggested the formation of Zn–O–Si bonds at the interface between the ZnO nanoparticles and the silica matrix. Our more particular results support the opinions expressed in the work of Yao *et al* [11] and Cannas *et al* [7]: they suggested that Si–O–Zn bonds can be formed in sol–gel ZnO–SiO$_2$.

The interface between the ZnO particles and SiO$_2$ matrix may enhance the UV emission by two possible mechanisms.

One possible mechanism is modifying the surface nature of the ZnO nanoparticles. Studies have shown that the luminescence efficiency of nanoparticles is strongly dependent on the nature of the surface, because small particles have a large surface-to-volume ratio. In the case of ZnO nanoparticles, surface states such as dangling bonds are usually involved in non-radiative processes, while O^{2-} ions provide a critical pathway for the visible emission band [4, 23–25]. Embedding the ZnO nanoparticles in a SiO$_2$ matrix will reduce the density of surface dangling bonds and O^{2-} ions via Zn–O–Si, so reducing the probability of non-radiative and visible emission; in contrast, the UV emission probability will be increased. This passivation mechanism may contribute partly to the UV PL enhancement.

Another possible mechanism via which the interface may contribute for the UV PL enhancement is by creation of interface states where carriers can be trapped and recombine to emit UV light. As demonstrated previously, the net charge of the Zn atom in the Zn–O–Si bond is positive. According to the general theory of defects, a positive centre in ZnO produces an attractive defect potential, attracting levels of the conduction band into the band gap and creating a donor state [26]. Due to the weak attractive potential, the Zn–O–Si interface state is shallow as compared with the ZnO:V$_O$ and ZnO:Zn$_I$ states. As a result, the energy level of the donor state created by Zn–O–Si may shift to 3.26 eV (380 nm) and act as a luminescence
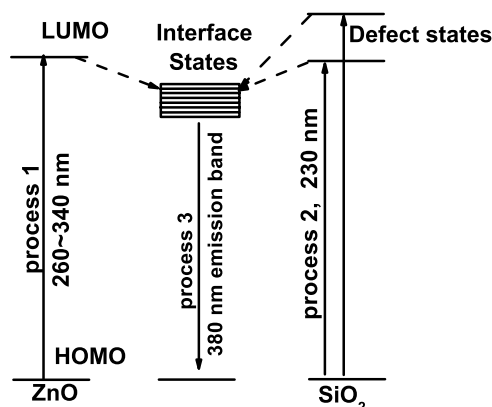
Figure 5. Schematic diagrams of the excitation and emission processes for the 380 nm band in ZnO–SiO$_2$ nanocomposites. Processes 1 and 2 correspond to the excitation processes with 260–340 nm light and 230 nm light respectively; process 3 corresponds to the emission processes for the 380 nm band.

centre for the 380 nm band; i.e., carriers excited in ZnO and SiO$_2$ may be trapped at the interface states and consequently recombine to emit a band at 380 nm. Because of the large interface-to-volume ratio in the nanocomposites, this process is greatly enhanced, resulting in enhancement of the UV emission efficiency.

In addition to the effect of the interface, the nanocomposite structure may contribute to the UV PL enhancement via enhancing the excitation process in the SiO$_2$ matrix and the luminescence process in the ZnO nanoparticles. In the nanocomposites, some of the carriers excited in the SiO$_2$ matrix may tunnel to the ZnO–SiO$_2$ interface or to ZnO nanoparticles and recombine, enhancing the UV band. On the other hand, SiO$_2$ provides a good coverage of the ZnO surface and may act as an energetic barrier preventing the escape of photogenerated carriers to outside the confined ZnO nanoparticles. However, more research is needed to elucidate the details.

On the basis of the above discussion, we illustrate the tentative excitation and emission processes of the 380 nm UV band in figure 5. First, a large number of carriers are excited in ZnO and SiO$_2$ via processes 1 and 2. Then some of the excited carriers are trapped at the interface and consequently recombine, emitting the band at 380 nm (process 3), while other excited carriers may recombine in the SiO$_2$ matrix and/or in ZnO nanoparticles, resulting in the 350 and 470 nm emission, as well as the band at 380 nm. All these processes may contribute to the enhancement of the UV PL in the nanocomposites.

4. Conclusions

In conclusion, the luminescence intensity of the UV emission in ZnO–SiO$_2$ nanocomposites prepared by the sol–gel method was much higher than that of sol–gel pure ZnO. The shift of $E_{B,2P}$, $E_{k,LMM}$, the Auger parameter, and E_{3d} for Zn in the composite are ascribed to the formation of Si–O–Zn at the ZnO–SiO$_2$ interface. New energy states are formed due to the presence of Zn–O–Si bonds at the interface. The PLE results show that both the ZnO nanoparticles and the SiO$_2$ matrix in the nanocomposites contribute to the luminescence process. A luminescence model concerning the contribution of the ZnO nanoparticles, SiO$_2$ matrix, and ZnO–SiO$_2$ interface is suggested to explain the PL enhancement effect.

Acknowledgments

References

[1] Zhang W H, Shi J L, Wang L Z and Yan D S 2000 *Chem. Mater.* **12** 1408
[2] Shi G, Mo C M, Cai W L and Zhang L D 2000 *Solid State Commun.* **115** 253
[3] Mo C M, Li Y H, Liu Y S, Zhang Y and Zhang L D 1998 *J. Appl. Phys.* **83** 4389
[4] Li J F, Yao L Z, Ye C H, Mo C M, Cai W L, Zhang Y and Zhang L D 2001 *J. Cryst. Growth* **223** 535
[5] Wang Y W, Zhang L D, Wang G Z, Peng X S, Chu Z Q and Liang C H 2002 *J. Cryst. Growth* **234** 171
[6] Guo L, Cheng J X, Li X Y, Yan Y J, Yang S H, Yang C L, Wang J N and Ge W K 2001 *Mater. Sci. Eng.* C **16** 123
[7] Cannas C, Casu M, Lai A, Musinu A and Piccaluga G 1999 *J. Mater. Chem.* **9** 1765
[8] Fujihara S, Naito H and Kimura T 2001 *Thin Solid Films* **389** 227
[9] Service R F 1997 *Science* **276** 895
[10] Sekiguchi T, Ohashi N and Terada Y 1997 *Defects Semicond.* **258** 1371
[11] Yao B D, Shi H Z, Bi H J and Zhang L D 2000 *J. Phys.: Condens. Matter* **12** 6265
[12] Sakohara S, Tickanen L D and Anderson M A 1992 *J. Phys. Chem.* **96** 11086
[13] Yang P, Lu M K, Song C F, Liu S W, Yuan D R, Xu D, Gu F, Cao D X and Chen D H 2002 *Inorg. Chem. Commun.* **5** 482
[14] Nyffenegger R M, Craft B, Shaaban M, Gorer S, Erley G and Penner R M 1998 *Chem. Mater.* **10** 1120
[15] Guo Lin, Yang Shihe, Yang Chunlei, Yu Ping, Wang Jiannong, Ge Weikun and Wong G K L 2000 *Appl. Phys. Lett.* **76** 2901
[16] Anedda A, Carbonaro C M, Corpino R and Raga F 1998 *Nucl. Instrum. Methods* B **141** 719
[17] Deroubaix G and Marcus P 1992 *Surf. Interface Anal.* **18** 39
[18] Futsuhara M, Yoshioka K and Takai O 1998 *Thin Solid Films* **322** 274
[19] Mikheeva E P, Koshcheev S V, Ruzankin S P, Zhidomirov G M, Leontiev S A, Devyatov V G and Cherkashin A E 1998 *J. Electron Spectrosc.* **94** 59
[20] Leontiev S A, Koshcheev S V, Devyatov V G, Cherkashin A E and Mikheeva E P 1997 *J. Struct. Chem.* **38** 725
[21] Mikheeva E P, Zhidomirov G M, Ruzankin S F, Leontiev S A, Devyatov V G, Koshcheev S V and Cherkashin A E 1997 *J. Struct. Chem.* **38** 732
[22] Zwicker G and Jacobi K 1985 *Solid State Commun.* **54** 701
[23] van Dijken A, Meulenkamp E A, Vanmaekelbergh D and Meijerink A 2000 *J. Lumin.* **87–89** 454
[24] van Dijken A, Makkinje J and Meijerink A 2001 *J. Lumin.* **92** 323
[25] van Dijken A, Meulenkamp E A, Vanmaekelbergh D and Meijerink A 2000 *J. Lumin.* **90** 123
[26] Sun Y M, Xu P S, Shi C S, Xu F Q, Pan H B and Lu E D 2001 *J. Electron Spectrosc.* **114–116** 1123